e-ISSN: 3089-5081 | p-ISSN: 1979-8911
Vol. 14 No. 2 December 2025: 62-70
DOI: 10.15575/istek.v14i2.2447

Numerical Simulation of Fluid Flow on An Open Channel with Parabolic Cross-section

Elvi Syukrina Erianto[1], Nadya Zulfani Aprilia[2], Mia Siti Khumaeroh[3]

[1,2,3] Mathematics Department, UIN Sunan Gunung Djati Bandung, Indonesia

Article Info

Article history:

Received
Revised
Accepted

Keywords:

Finite Volume Method
Numerical simulation
Open channel
Parabolic cross-section
Shallow Water Equation

ABSTRACT

Water is a vital resource whose movement is influenced by various factors such as gravity and frictional force. The cross-sectional shape of a channel can significantly influence the friction force,consequently, affect the flow characteristics. One of the interesting cross-sectional shapes to analyze is parabolic because of its unique geometric properties. This study aims to conduct a numerical simulation of open channel flow within a parabolic cross-section using a modified Shallow Water Equation and the Finite Volume Method implemented with a staggered grid scheme. The mathematical model used takes into account the influence of the parabolic shape through the calculation of Manning's friction, which depends on the hydraulic radius. The Shallow Water Equations, consisting of the continuity and momentum equations, are solved numerically through spatial and temporal discretization. The simulations are perfomed using Scilab to generate visualizations of the water depth and flow velocity distribution under various geometric conditions. This study produces simulations of one-dimensional (1D) and two-dimensional (2D) dam-break flows with a parabolic cross section and compares them with the rectangular cross-section. The simulation results show that the finite volume method with the staggered grid scheme provides stable solutions and is capable of accurately describing the flow behavior across different channel geometries .

Corresponding Author:

Elvi Syukrina Erianto,
Mathematics Department, Faculty of Science & Technology, UIN Sunan Gunung Djati Bandung
Jl. A. H. Nasution No. 105, Cibiru, Bandung, Indonesia. 40614
Email : elvise@uinsgd.ac.id

1. INTRODUCTION

The study about fluid flow on an open channel is so important in designing some infrastructures around a river or canal such as irrigation or flood mitigation. Open channel geometry, including its cross-sectional shape and slope, can affect the characteristic of fluid flow [1]. One of the interesting channel geometry is an open channel with parabolic cross-section because of the analytical simplicity and its application in drainase system [2]. The parabolic geometry offers higher hydraulic efficiency and reduces the risk of sedimentation because its shape helps maintain higher flow velocity even at low discharge[3].

To model the fluid flow in an open channel mathematically, researchers often use the Shallow Water Equation(SWE) with some diffetent assumpsions based on the case, i.e. [4],[5],[6],[7]. SWE consists of two equations. They are continuity equation and momentum concervative equation. Several researchers have examined the fluid flow on an open channel with different cross-sectional shapes such as trapezoidal, parabolic, and circular[8],[3],[9]. These cross-sectional shapes influence the mathematical models used, particularly because channel geometry can affect the friction force. Hence, friction term in the model, i.e Manning friction term, often need to be modified.

The analytical solutions of SWE is not always easy to be found, moreover if nonlinear terms are involved. Therefore, numerical approaches are required to obtain the approximate solution. Various numerical methods have been applied, including finite difference and Finite Volume Methods(FVM).

FVM is suitable for the discontinious cases. In FVM, many schemes can be applied, such as WENO, Godunov-type, or staggered scheme[10]. WENO scheme has the higher accuracy but more complex and has a complicated stencil structure[7]. Staggered grid scheme is well balanced and easier to implement because it does not need Riemann solver[11].

In this study, we develop numerical simulations of fluid flow on an open channel with parabolic cross-section in both 1D and 2D, using the FVM with a staggered grid scheme. The changes in water depth and flow velocity are analyzed, and the fluid characteristics of fluid in a channel with parabolic and rectangular cross-section are compared.

2. Wave Model and Numerical Scheme

In this paper, we discuss a fluid flow model for an open channel with parabolic cross-section and solve it numerically. Consider the inviscid fluid with water depth $h(x,y,t)$, horizontal velocity in x and y direction respectively $u(x,y,t)$ and $v(x,y,t)$, friction force S_f, gravitational acceleration g, and bottom topography z. The 2D SWE is employed and expressed as follows[12].

$$\frac{\partial h}{\partial t}+\frac{\partial (hu)}{\partial x}+\frac{\partial (hv)}{\partial y}=0 \tag{1}$$

$$\frac{\partial (hu)}{\partial t}+\frac{\partial}{\partial x}\left(hu^2+\frac{1}{2}gh^2\right)=-\frac{\partial (huv)}{\partial y}-gh\frac{\partial z}{\partial x}-ghS_f \tag{2}$$

$$\frac{\partial (hv)}{\partial t}+\frac{\partial}{\partial y}\left(hv^2+\frac{1}{2}gh^2\right)=-\frac{\partial (huv)}{\partial x}-gh\frac{\partial z}{\partial y}-ghS_f \tag{3}$$

The Manning friction force is used and expressed by (4).

$$S_f = R\cdot n^2\cdot u|u| \tag{4}$$

Where R is hydraulic radius and n is Manning coefficient. Consider the width of the channel is b, so the parabolic cross section is modeled by

$$A=\frac{2}{3}hb \tag{5}$$

The hydraulic radius becomes the following form:

$$R=\frac{2b^2\cdot h(x,t)}{3b^2+8h^2(x,t)} \tag{6}$$

Eq. (6) is substituted to Eq. (4), hence we get the Manning friction force as follows.

$$S_f=\frac{2b^2\cdot h(x,t)}{3b^2+8h^2(x,t)}\cdot n^2\cdot u|u| \tag{7}$$

The 2D SWE in Eq. (1)-(3) is approximated by Finite Volume Method(FVM) with staggered grid scheme. Consider the spatial domain $[0,L]$ and $[0,M]$. Then, they are discretized by Δx and Δy into Nx and N_y grids. In staggered grid scheme, mass and momentum are calculated in different cell to improve accuracy and stability of the calculation[11]. Let the grids in (i,j) are denoted by x_i, y_j, with $i=0,1,\dots,N_x$ and $j=0,1,\dots,N_y$, called the full grid. Besides, the grids are denoted by $x_{i+\frac{1}{2}}, y_j$ and $x_i, y_{j+\frac{1}{2}}$, with $i=0,1,\dots,N_x$ and $j=0,1,\dots,N_y$, called the half grid. So, the water depth (h) is calculated in full grid, while the horizontal velocities (u and v) are calculated in half grid by $x_{i+\frac{1}{2}}, y_j$ and $x_i, y_{j+\frac{1}{2}}$. The time domain $[0,T]$ is divided into N_t grids, hence the time in n-th step $t_n=n\Delta t$. The approximation of h in grid (i,j) at time t_n is denoted by $h_{i,j}^n=h(x_i,y_j,t_n)$, and so are $u_{i+\frac{1}{2},j}^n=u\left(x_{i+\frac{1}{2}},y_j,t_n\right)$ and $v_{i,j+\frac{1}{2}}^n=v\left(x_i,y_{j+\frac{1}{2}},t_n\right)$.

The mass concervation equation (1) is approximated as follows.

$$\frac{h_{i,j}^{n+1}-h_{i,j}^{n}}{\Delta t}+\left(\frac{p_{i+\frac{1}{2},j}^{n}-p_{i-\frac{1}{2},j}^{n}}{\Delta x}\right)+\left(\frac{q_{i,j+\frac{1}{2}}^{n}-q_{i,j-\frac{1}{2}}^{n}}{\Delta y}\right)=0 \tag{8}$$

where $p(x,y,t)$ and $q(x,y,t)$ are flow rate, defined as:

$$\begin{aligned} p_{i+\frac{1}{2},j}^{n} &= {}^{*}h_{i+\frac{1}{2},j}^{n}\, u_{i+\frac{1}{2},j}^{n} \\ q_{i,j+\frac{1}{2}}^{n} &= {}^{*}h_{i,j+\frac{1}{2}}^{n}\, v_{i,j+\frac{1}{2}}^{n} \end{aligned} \tag{9}$$

The first-order upwind scheme is used to calculated ${}^{*}h_{i+\frac{1}{2},j}^{n}$ and ${}^{*}h_{i,j+\frac{1}{2}}^{n}$, as follows.

$$\begin{aligned} {}^{*}h_{i+\frac{1}{2},j}^{n} &= \begin{cases} h_{i,j}^{n}, & if\ u_{i+\frac{1}{2},j}^{n} \geq 0 \\ h_{i+1,j}^{n}, & if\ u_{i+\frac{1}{2},j}^{n} < 0 \end{cases} \\ {}^{*}h_{i,j+\frac{1}{2}}^{n} &= \begin{cases} h_{i,j}^{n}, & if\ v_{i,j+\frac{1}{2}}^{n} \geq 0 \\ h_{i,j+1}^{n}, & if\ v_{i,j+\frac{1}{2}}^{n} < 0 \end{cases} \end{aligned} \tag{10}$$

Eq. (2) is approximated by:

$$\begin{aligned} &\frac{\bar{h}_{i+\frac{1}{2},j}^{n+1}\, u_{i+\frac{1}{2},j}^{n+1}-\bar{h}_{i-\frac{1}{2},j}^{n}\, u_{i-\frac{1}{2},j}^{n}}{\Delta t}+\left(\frac{\bar{q}_{i+\frac{1}{2},j+\frac{1}{2}}^{n}\, u_{i+\frac{1}{2},j+\frac{1}{2}}^{n}-\bar{q}_{i+\frac{1}{2},j-\frac{1}{2}}^{n}\, u_{i+\frac{1}{2},j-\frac{1}{2}}^{n}}{\Delta y}\right) \\ &\quad+\left(\frac{\bar{p}_{i+1,j}^{n}\, u_{i+1,j}^{n}-\bar{p}_{i,j}^{n}\, u_{i,j}^{n}}{\Delta x}\right)+\frac{1}{2}g\left(\left(h_{i+1,j}^{n+1}\right)^{2}-\left(h_{i,j}^{n+1}\right)^{2}\right) \\ &\quad+g h_{i+1,j}^{n+1}\left(\frac{z_{i+1,j}-z_{i,j}}{\Delta x}\right)+g\, {S_f}_{i+\frac{1}{2},j}^{n}=0 \end{aligned} \tag{11}$$

where $\bar{h}_{i+\frac{1}{2},j}^{n+1}$, $\bar{q}_{i+\frac{1}{2},j+\frac{1}{2}}^{n}$, and $\bar{p}_{i,j}^{n}$ are calculated as the average of the values in two grids at one cell.

$$\begin{aligned} \bar{h}_{i+\frac{1}{2},j}^{n+1} &= \frac{1}{2}\left(h_{i,j}^{n}+h_{i+1,j}^{n}\right) \\ \bar{q}_{i+\frac{1}{2},j+\frac{1}{2}}^{n} &= \frac{1}{2}\left(q_{i+1,j+\frac{1}{2}}^{n}+q_{i,j+\frac{1}{2}}^{n}\right) \\ \bar{p}_{i,j}^{n} &= \frac{1}{2}\left(p_{i-\frac{1}{2},j}^{n}+p_{i+\frac{1}{2},j}^{n}\right) \end{aligned} \tag{12}$$

Eq. (3) is approximated by:

$$\begin{aligned} &\frac{\bar{h}_{i,j+\frac{1}{2}}^{n+1}\, v_{i,j+\frac{1}{2}}^{n+1}-\bar{h}_{i,j-\frac{1}{2}}^{n}\, v_{i,j-\frac{1}{2}}^{n}}{\Delta t}+\left(\frac{\bar{p}_{i+\frac{1}{2},j+\frac{1}{2}}^{n}\, v_{i+\frac{1}{2},j+\frac{1}{2}}^{n}-\bar{p}_{i-\frac{1}{2},j+\frac{1}{2}}^{n}\, v_{i-\frac{1}{2},j+\frac{1}{2}}^{n}}{\Delta x}\right) \\ &\quad+\left(\frac{\bar{q}_{i,j+1}^{n}\, v_{i,j+1}^{n}-\bar{q}_{i,j}^{n}\, v_{i,j}^{n}}{\Delta y}\right)+\frac{1}{2}g\left(\left(h_{i,j+1}^{n+1}\right)^{2}-\left(h_{i,j}^{n+1}\right)^{2}\right) \\ &\quad+g h_{i,j+1}^{n+1}\left(\frac{z_{i,j+1}-z_{i,j}}{\Delta x}\right)+g\, {S_f}_{i,j+\frac{1}{2}}^{n}=0 \end{aligned} \tag{13}$$

where $\bar{h}_{i,j+\frac{1}{2}}^{n+1}$, $\bar{p}_{i+\frac{1}{2},j+\frac{1}{2}}^{n}$, and $\bar{q}_{i,j}^{n}$ are also calculated as the average of the values in two grids at one cell.

$$\begin{aligned} \bar{h}_{i,j+\frac{1}{2}}^{n+1} &= \frac{1}{2}\left(h_{i,j}^{n}+h_{i+1,j}^{n}\right) \\ \bar{q}_{i,j}^{n} &= \frac{1}{2}\left(q_{i,j+\frac{1}{2}}^{n}+q_{i,j-\frac{1}{2}}^{n}\right) \end{aligned} \tag{14}$$

$$\bar{p}^{n}_{i+\frac{1}{2},j+\frac{1}{2}} = \frac{1}{2}\left(p^{n}_{i+\frac{1}{2},j+1} + p^{n}_{i+\frac{1}{2},j}\right)$$

The explicit form of (8), (11), (13) are expressed in the equations as follows.

$$h^{n+1}_{i,j} = h^{n}_{i,j} - \frac{1}{\Delta t}\left(\frac{p^{n}_{i+\frac{1}{2},j} - p^{n}_{i-\frac{1}{2},j}}{\Delta x}\right) - \frac{1}{\Delta t}\left(\frac{q^{n}_{i,j+\frac{1}{2}} - q^{n}_{i,j-\frac{1}{2}}}{\Delta y}\right) \tag{15}$$

$$\begin{aligned} u^{n+1}_{i+\frac{1}{2},j} = {} & \frac{1}{\bar{h}^{n+1}_{i+\frac{1}{2},j}} \bar{h}^{n}_{i-\frac{1}{2},j}\, u^{n}_{i-\frac{1}{2},j} - \frac{1}{\Delta t}\left(\frac{\bar{q}^{n}_{i+\frac{1}{2},j+\frac{1}{2}}\, u^{n}_{i+\frac{1}{2},j+\frac{1}{2}} - \bar{q}^{n}_{i+\frac{1}{2},j-\frac{1}{2}}\, u^{n}_{i+\frac{1}{2},j-\frac{1}{2}}}{\Delta y}\right) \\ & - \frac{1}{\Delta t}\left(\frac{\bar{p}^{n}_{i+1,j}\, u^{n}_{i+1,j} - \bar{p}^{n}_{i,j}\, u^{n}_{i,j}}{\Delta x}\right) - \frac{1}{2\Delta t} g\left(\left(h^{n+1}_{i+1,j}\right)^2 - \left(h^{n+1}_{i,j}\right)^2\right) \\ & - \frac{1}{\Delta t} g h^{n+1}_{i+1,j}\left(\frac{z_{i+1,j} - z_{i,j}}{\Delta x}\right) - \frac{g}{\Delta t}\, {S_f}^{n}_{i+\frac{1}{2},j} \end{aligned} \tag{16}$$

$$\begin{aligned} v^{n+1}_{i,j+\frac{1}{2}} = {} & \frac{1}{\bar{h}^{n+1}_{i,j+\frac{1}{2}}} \bar{h}^{n}_{i,j-\frac{1}{2}}\, v^{n}_{i,j-\frac{1}{2}} - \frac{1}{\Delta t}\left(\frac{\bar{p}^{n}_{i+\frac{1}{2},j+\frac{1}{2}}\, v^{n}_{i+\frac{1}{2},j+\frac{1}{2}} - \bar{p}^{n}_{i-\frac{1}{2},j+\frac{1}{2}}\, v^{n}_{i-\frac{1}{2},j+\frac{1}{2}}}{\Delta x}\right) \\ & - \frac{1}{\Delta t}\left(\frac{\bar{q}^{n}_{i,j+1}\, v^{n}_{i,j+1} - \bar{q}^{n}_{i,j}\, v^{n}_{i,j}}{\Delta y}\right) - \frac{1}{2\Delta t} g\left(\left(h^{n+1}_{i,j+1}\right)^2 - \left(h^{n+1}_{i,j}\right)^2\right) \\ & - \frac{1}{\Delta t} g h^{n+1}_{i,j+1}\left(\frac{z_{i,j+1} - z_{i,j}}{\Delta y}\right) - \frac{g}{\Delta t}\, {S_f}^{n}_{i,j+\frac{1}{2}} \end{aligned} \tag{17}$$

Eq. (15)-(17) are the numerical solution of 2D SWE Eq. (1)-(3). The same way can be implemented into 1D SWE by ommiting the y-term.

3. RESULT AND DISCUSSION

In this section, we simulate the model of 1D SWE and 2D SWE with dam-break case study then analyze the differences beetwen parabolic cross section and rectangular cross section.

1D Dam-Break Simulation

In this case, let the channel width is constant $b(x) = 1$ and gravitational acceleration is 9.81. The spacial and time domain, respectively are $0 \le x \le 200$ and $0 \le t \le 10$, divided by the step size $\Delta x = 0.25$ and $\Delta t = 0.005\Delta x$. The initial condition of the dam-break for the water level at time $t = 0$, as follows.

$$h(x,0) = \begin{cases} 10, & jika\ x \le 100 \\ 2, & jika\ x > 100 \end{cases} \tag{18}$$

The initial horizontal velocity is $u(x,0) = 0$, with the hardwall boundary conditions as follows.

$$\begin{aligned} u(0,t) &= u(200,t) = 0 \\ h(0,t) &= 10, \qquad h(200,t) = 2 \end{aligned} \tag{19}$$

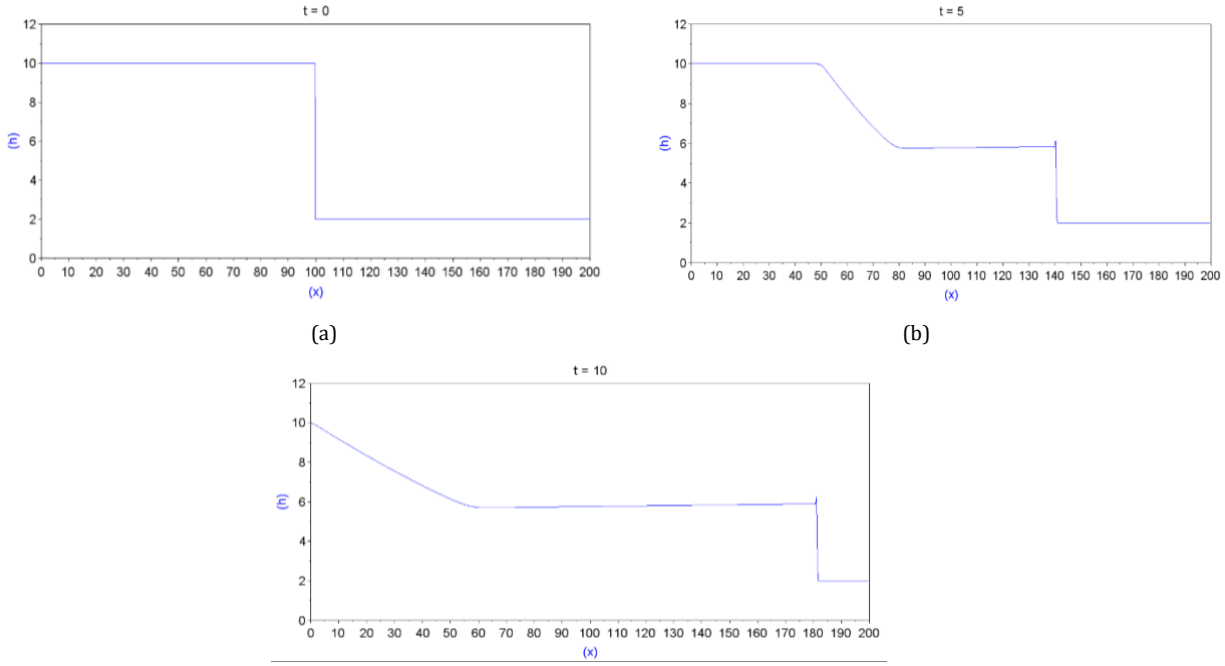

Figure 1. The result of 1D dam-break numerical simulation on parabolic cross section open channel at different time. (a) at $t = 0$, (b) at $t = 5$, (c) at $t = 10$.

The result of simulation, seen at Fig. 1, shows that the fluid flow propagates to the right. The water depth at the left side decreases over time but contrary with the right side. At $t = 10$, the depth distribution becomes more uniform, indicating a gradual spreading of the fluid mass.

2D Dam-Break Simulation

Let the channel width is constant $b(x) = 100$ and gravitational acceleration is 9.81. The cross section is parabolic with maximum depth $d_0 = 20$. The spacial and time domain, respectively are $0 \leq x \leq 500, 0 \leq y \leq 500,$ and $0 \leq t \leq 10,$ divided by the step size $\Delta x = 10, \Delta y = 10$ and $\Delta t = 0.01$. The initial condition of the dam-break for the water level at time $t = 0$, as follows.

$$\eta(x, y, 0) = \begin{cases} 0, & jika\ x \leq 250 \\ 10, & jika\ x > 250 \end{cases} \quad (20)$$

The initial horizontal velocity is $u(x, y, 0) = 0$, with the hardwall boundary conditions as follows.

$$u(0, y, t) = u(500, y, t) = v(x, 0, t) = v(x, 500, t) = 0 \quad (21)$$

The result for 2D dam-break numerical simulation over an open channel with parabolic cross-section can be seen at Fig.2.

The simulation results show that the water begins to flow and fill the right side of the channel after the dam breaks. The water surface shape follows the parabolic contour of the channel bed, with accumulation at the lowest point.

Comparison between Dam-break Simulation Over An Open Channel with Parabolic Cross Section and Rectangular Cross Section

In comparing dam-break flow over an open channel with parabolic and rectangular cross section, we employ 1D and 2D SWE. The velocity and water depth are analyzed. The comparison in 1D SWE can be seen in Fig. 3 and Fig. 4.

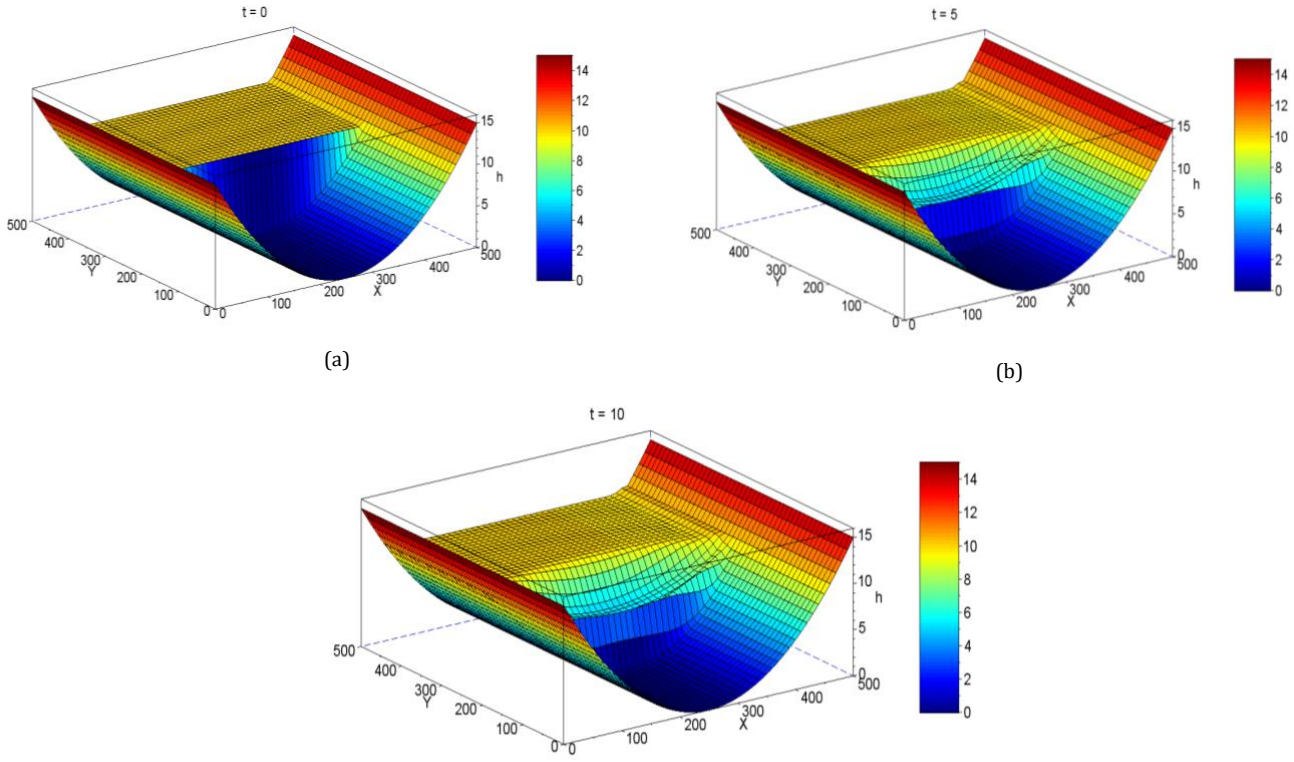

(a) (b) (c)

Figure 2. The result of 2D dam-break numerical simulation on parabolic cross section open channel at different time. (a) at $t = 0$, (b) at $t = 5$, (c) at $t = 10$.

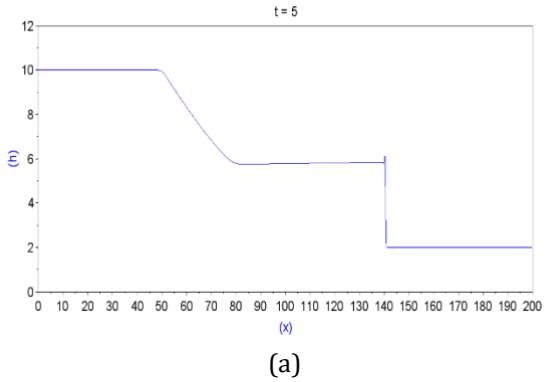

(a)

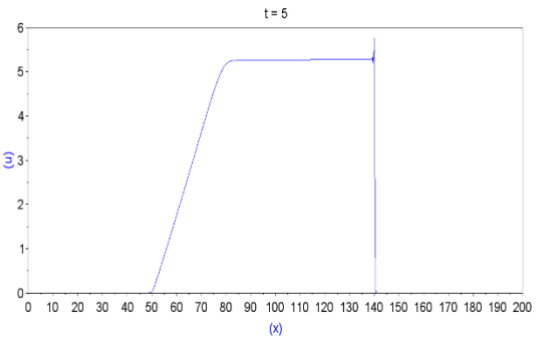

(b)

Figure 3. The result of 1D dam-break numerical simulation on parabolic cross section open channel at time $t = 5$. (a) for water depth h, (b) for horizontal velocity u

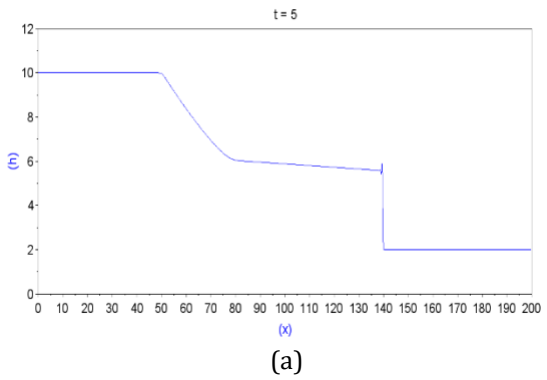

(a)

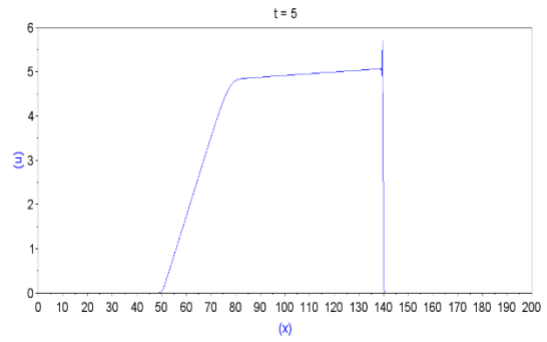

(b)

Figure 4. The result of 1D dam-break numerical simulation on rectangular cross section at time $t = 5$. (a) for water depth h, b) for horizontal velocity u

Tabel 1 presents the value of h and u at spesific points in the simulatin domain for each geometry.

Tabel 1. The comparison of h values at time $t = 5$

x	h	
	Parabolic	Rectangular
0	10	10
45	9,966	9,966
50	9,265	9,269
55	8,514	8,531
60	7,805	7,842
65	7,141	7,203
70	6,535	6,629
75	6,042	6,192
80	5,837	6,040
85	5,824	6,001
90	5,820	5,964

x	h	
	Parabolic	Rectangular
95	5,817	5,927
100	5,813	5,889
105	5,809	5,852
110	5,805	5,814
115	5,801	5,775
120	5,797	5,737
125	5,794	5,698
130	5,790	5,659
135	5,786	5,620
140	5,782	5,581
145	2	2

Based on Table 1, the simulation results show differences in the water depth h between an open channel with parabolic and rectangular cross section at time $t = 5$ at some positions x. At position $x = 45$ to $x = 110$, the water dept in the parabolic channel is lower because the flow is concentrated in the center of the channel. Contrary with that, at position $x = 115$ to $x = 140$ the water depth in parabolic channel is higher due to a smoother flow distribution.

Tabel 2. The comparison of u values at time $t = 5$

x	u	
	Parabolic	Rectangular
0	0	0
45	0	0
50	0,033	0,033
55	0.822	0,817
60	1,731	1,707
65	2,661	2,601
70	3,605	3,489
75	4,519	4,309
80	5,158	4,793
85	5,259	4,854
90	5,261	4,874

x	u	
	Parabolic	Rectangular
95	5,263	4,914
100	5,265	4,934
105	5,267	4,954
110	5,269	4,973
115	5,272	4,993
120	5,274	5,012
125	5,276	5,032
130	5,278	5,051
135	5,280	4,943
140	5,097	4,899
145	0	0

The simulation in 2D is also compared between the parabolic and rectangular. Based on the data that are used in 2D dam-break simulation above, we get the comparison of water profile, seen in Fig. 5.

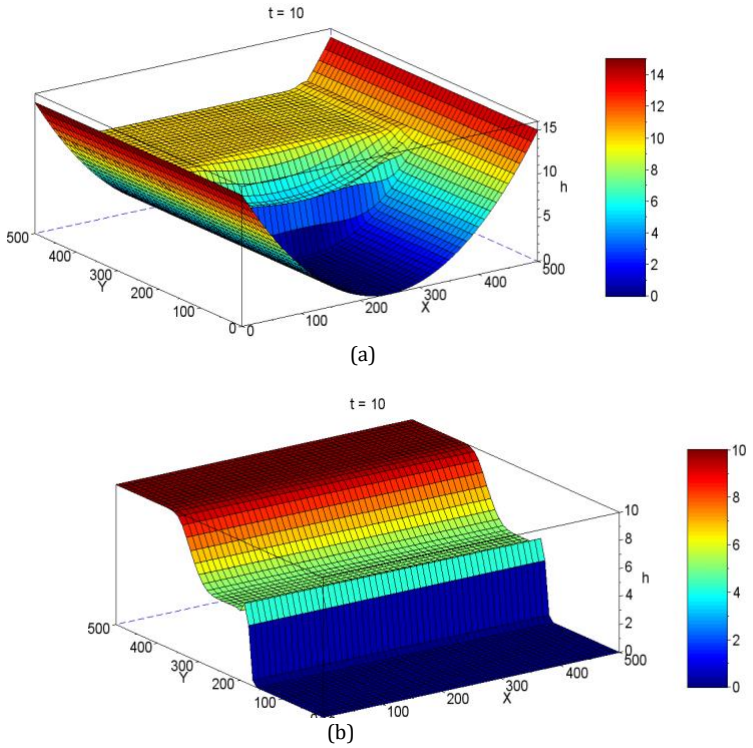

Figure 1. The result of 2D dam-break simulation at time t=10. (a) parabolic cross section , (b) recyangular croo section

In the 2D simulation, the parabolic channel produces a curved water surface that spread following the shape of bottom topography. In contrast, the rectangular channel shows a more uniform surface, with limited lateral spreading due to its flat, sharp-edged bottom. These differences confirm that channel geometry has a significant impact on flow characteristics, influencing the velocity and water depth distribution.

4. CONCLUSION

This study shows that the modified SWE on an open channel can accurately describe the flow in a parabolic channel. The numerical method used is stable and works well for complex shapes. In the 1D dam-break case, the water level decrease gradually upstream and becomes more even as the flow moves downstream. In 2D case, the water spreads folloving the curved channel bed and collects at the lowest poin, showing that channel shape strongly affects the flow. Overall, the open channel with parabolic cross section geometry can produces faster and smoother flow with a mor even water surface, while the he open channel with rectangular cross section geometry leads to slower flow and sharper changes in water depth.

REFERENCES

[1] C. Qiu, S. Liu, J. Huang, W. Pan, and R. Xu, "Influence of Cross-Sectional Shape on Flow Capacity of Open Channels," *Water*, vol. 15, no. 10, p. 1877, 2023.

[2] Y.-C. Han and S. M. Easa, "New and improved three and one-third parabolic channel and most efficient hydraulic section," *Can. J. Civ. Eng.*, vol. 44, no. 5, pp. 387–391, 2017.

[3] F. K. Rotich, J. S. Maremwa, and J. Kipchirchir, "Mathematical modeling of flow of fluids in an open channel of parabolic cross-section," 2021.

[4] P. García-Navarro, J. Murillo, J. Fernández-Pato, I. Echeverribar, and M. Morales-Hernández, "The shallow water equations and their application to realistic cases," *Environ. Fluid Mech.*, vol. 19, no. 5, pp. 1235–1252, 2019.

[5] Q. Liang, "Simulation of shallow flows in nonuniform open channels," 2008.

[6] T.-J. Chang, H.-M. Kao, K.-H. Chang, and M.-H. Hsu, "Numerical simulation of shallow-water dam break flows in open channels using smoothed particle hydrodynamics," *J. Hydrol.*, vol. 408, no. 1–2, pp. 78–90, 2011.

[7] N. Črnjarić-Žic, S. Vuković, and L. Sopta, "Balanced finite volume WENO and central WENO schemes for the shallow water and the open-channel flow equations," *J. Comput. Phys.*, vol. 200, no. 2, pp. 512–548, 2004.

[8] P. K. Marangu, E. K. Mwenda, and D. M. Theuri, "Modeling open channel fluid flow with trapezoidal cross section and a segment base," 2016.

[9] M. N. Kinyanjui, D. P. Tsombe, J. K. Kwanza, and K. Gaterere, "Modeling fluid flow in open channel with circular cross-section," *J. Agric. Sci. Technol.*, vol. 13, no. 2, pp. 78–89, 2011.

[10] E. Dick, "Introduction to finite volume methods in computational fluid dynamics," in *Computational fluid dynamics*, Springer, 2009, pp. 275–301.

[11] S. Mungkasi, I. Magdalena, S. R. Pudjaprasetya, L. H. Wiryanto, and S. G. Roberts, "A staggered method for the shallow water equations involving varying channel width and topography," *Int. J. Multiscale Comput. Eng.*, vol. 16, no. 3, pp. 231–244, 2018, doi: 10.1615/IntJMultCompEng.2018027042.

[12] M. Zijlema, "Computational modelling of flow and transport," *Lect. notes*, 2015.